

cPLA2 inhibition affects the relationship between vascular function and structure in a patient-derived breast cancer model: a correlation study of DCE-MRI vs. micro-CT

Eugene Kim¹, Astrid Jullumstrø Feuerherm^{2,3}, Berit Johansen^{2,3}, Olav Engebraaten⁴, Gunhild Mari Mælandsmo⁴, Tone Frost Bathen¹, and Siver Andreas Moestue¹
¹MR Cancer Group, Department of Circulation and Medical Imaging, Norwegian University of Science and Technology, Trondheim, Norway, ²Department of Biology, Norwegian University of Science and Technology, Trondheim, Norway, ³Avexxin AS, Trondheim, Norway, ⁴Department of Tumor Biology, Institute for Cancer Research, Oslo University Hospital, Oslo, Norway

Target audience: Researchers and clinicians interested in imaging of tumor vasculature and anti-angiogenic therapy.

Purpose: Cytosolic phospholipase A2 (cPLA2) is upregulated in basal-like breast cancer (BLBC)¹ and plays an important role in breast carcinogenesis and angiogenesis². Thus, it is a potential target for anti-angiogenic therapy in BLBC. Dynamic contrast enhanced (DCE)-MRI is commonly used in clinical breast cancer trials to monitor anti-angiogenic treatment effects on vascular function, namely flow and permeability. The impact of vascular structure on DCE-MRI measurements is less emphasized. In this study, we used DCE-MRI and *ex vivo* micro-CT angiography to investigate the relationship between tumor vascular function and structure, and the effect of a cPLA2 inhibitor (AVX235, Avexxin AS) on this relationship, in a patient-derived breast cancer model.

Methods: Patient-derived BLBC xenografts (MAS98.12) were orthotopically implanted in 16 athymic nude mice, which were randomized into treatment (n=9) or control (n=7) groups. Once the tumors grew to ~170 mm³, the mice received daily i.p. injections of AVX235 (45 mg/kg) or an equal volume of DMSO. **MRI:** The tumors were scanned on a Bruker 7T preclinical MRI system the day before the start of treatment (day 0) and again on day 7 using the following sequences: 1) 3D FLASH: TE=3 ms, TR=13 ms, flip angle=30°, 4 averages, matrix=128×128×32, FOV=20×20×10 mm. 2) 2D RARE with variable repetition times for baseline T1 measurement: TE=13 ms, six TRs from 225 to 12000 ms, matrix=64×64, FOV=20×20 mm, slice thickness=0.6 mm, interslice gap= 0.3 mm, 4 slices. 3) Dynamic series of 200 2D RARE images: TE=7.5 ms, TR=300 ms, temporal resolution=4.8 s, same geometry as the T1 map. An intravenous bolus injection of gadodiamide (0.3 mmol/kg) was administered after the tenth baseline image. **μCT:** Immediately following the final MRI exam, the mice were sacrificed by pentobarbital overdose followed by intracardiac perfusion with Microfil® (Flow Tech, Inc., Carver, MA), an intravascular CT contrast agent. The tumors were excised, fixed in formalin for 48 h, and imaged on a Bruker Skyscan 1176 μCT system: 50 kV, 400 μA, 0.5 mm Al filter, 1020 ms exposure, 0.36° rotation step, 8 averages, 9 μm isotropic voxels.

Image processing: Tumor volumes of interest (VOI) were manually drawn on the 3D FLASH and μCT images. K^{trans} , v_e and v_p maps were computed from the DCE-MRI data acquired on day 7 using the extended Tofts model and a population-based arterial input function³. The μCT images were co-registered to the MRI by maximizing the correlation between the binary VOIs using a 9-parameter 3D affine transformation. Tumor vessels were segmented from the μCT images using a Hessian-based filtering method⁴. The DCE-MRI parametric maps were downsampled in-plane by averaging to an 8×8 matrix (blue grid, Fig. 1). Micro-CT fractional blood volume (FBV), vessel surface area (SA), mean distance to the nearest vessel (DNV), and mean vessel diameter were computed within each voxel of the 8×8 matrix. The spatial correlations between the DCE-MRI and μCT parameters were then measured for each tumor using the Pearson correlation coefficient, r . Two-tailed Mann-Whitney U tests ($\alpha=0.05$) were used to compare control and treated groups.

Results and discussion: There was no significant difference in median SA, vessel diameter, or any Tofts parameter between control and treated groups. FBV was significantly lower and median DNV greater in treated tumors. The co-registration correlation metrics ranged from 0.83 to 0.91 and were not different between groups. There was no statistically significant relationship between the accuracy of co-registration and the correlations between DCE-MRI and μCT parameters. For control tumors, there was good correlation between K^{trans} and SA (Table 1, Fig. 2a), which was expected since K^{trans} is a function of flow, permeability, and surface area. This correlation was weaker in treated tumors (Fig. 2d). In control tumors, v_p correlated well with FBV (Fig. 2c), but the correlation with SA was stronger (Table 1). This may be due to contributions of trans-endothelial water exchange on T1 relaxation enhancement. These correlations were also poorer in treated tumors. The generally weaker correlations in treated tumors suggests that AVX235 modulated the link between vascular structure and function and had a spatially heterogeneous effect on blood flow and/or vessel permeability, which may have decreased the accuracy of the Tofts model parameter estimates⁵. However, the correlation between v_e and DNV was similar for control and treated tumors, perhaps because v_e is relatively less related to the vasculature than K^{trans} and v_p . In addition, diffusion-weighted MRI indicated that AVX235 had little effect on tumor cellularity after one week of treatment (unpublished data). The correlation between v_e and DNV may be explained by the fact that regions farther away from the blood supply are likely less viable with lower cell density. Interestingly, there was no correlation between vessel diameter and the DCE-MRI parameters.

Conclusion: DCE-MRI measurements are complex functions of both vascular function and structure, and the relationship between these two aspects of tumor vasculature is still not fully understood. In this study, we showed that cPLA2 inhibition modulates this relationship and that the combination of DCE-MRI and μCT data contributed to an improved understanding of the underlying biology of DCE-MRI biomarkers for monitoring response to anti-angiogenic therapy.

References: 1. Grinde MT, et al. *Breast Cancer Res* 2014, 16:R5. 2. Wen ZH, et al. *Oncogene* 2013, 32(2):160-70. 3. Jensen LR, et al. *Cancer Biol Ther* 2007, 6(11):1810-6. 4. Kim E, et al. *Magn Reson Med* 2013, 70(4):1106-16. 5. Sourbron and Buckley. *Magn Reson Med* 2011, 66(3):735-45.

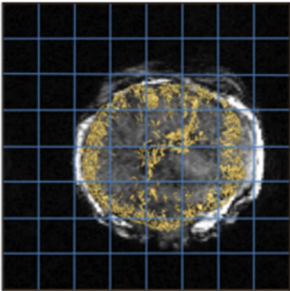


Fig. 1 Co-registered μCT vessels (yellow) overlaid on the 3D FLASH image of a representative breast tumor xenograft.

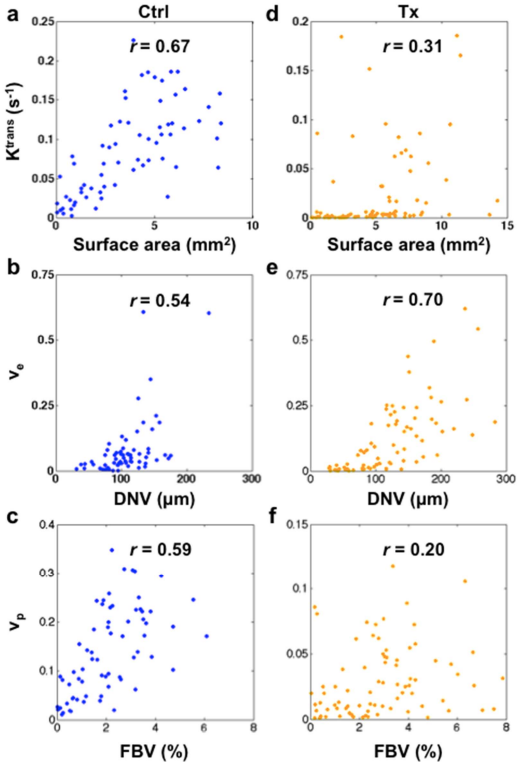


Fig. 2 Correlation plots of DCE-MRI vs. μCT parameters for a control tumor (a-c) and a treated tumor (d-f).

Table 1 Median Pearson correlation coefficients between DCE-MRI (columns) and μCT (rows) parameters (interquartile range in brackets). Column maximums are bolded, and row maximums are italicized.

	K^{trans}	v_e	v_p
FBV	0.51 [0.24, 0.65]	0.27 [0.22, 0.41]	0.59 [0.36, 0.68]
SA	0.67 [0.32, 0.75]	0.37 [0.30, 0.51]	0.7 [0.42, 0.78]
DNV	0.47 [0.19, 0.69]	0.52 [0.26, 0.70]	0.29 [0.21, 0.42]
Diameter	0.08 [0.02, 0.21]	0.04 [0.02, 0.27]	0.19 [0.08, 0.33]
FBV	0.2 [-0.07, 0.25]	0.2 [0.07, 0.26]	0.23 [0.08, 0.46]
SA	0.25 [-0.01, 0.35]	0.29 [0.21, 0.33]	0.33 [0.17, 0.53]
DNV	0.36 [0.27, 0.58]	0.51 [0.37, 0.62]	0.22 [0.03, 0.41]
Diameter	0.01 [-0.06, 0.12]	0.08 [-0.00, 0.13]	0.12 [-0.01, 0.22]